

## Flash sintering of metal-like ceramics: A short overview



Vincenzo M. Sglavo <sup>a,b,\*</sup>, Emanuele De Bona <sup>a</sup>, Isacco Mazo <sup>a,1</sup>

<sup>a</sup> Department of Industrial Engineering, University of Trento, via Sommarive 9, Trento, Italy

<sup>b</sup> INSTM, National Interuniversity Consortium of Materials Science and Technology, Trento Research Unit, Via G. Giusti 9, 50123, Firenze, Italy

### ARTICLE INFO

Handling Editor: Dr P. Vincenzini

**Keywords:**

Flash sintering  
Metal-like ceramics  
Tungsten carbide  
Zirconium diboride

### ABSTRACT

Flash sintering was officially discovered about fifteen years ago as a ground-breaking method to consolidate ceramics in very short time at furnace temperature much lower than that used for conventional sintering. Since then, it has been applied to several ceramics and composites with the common feature of being characterized by a negative temperature coefficient for resistivity while few attempts have been made on materials with metal-like electronic conduction. In the present overview the results of the investigation carried out in the last years aiming at consolidating tungsten carbide and zirconium diboride by flash sintering are reported and the conditions for inducing a thermal runaway phenomenon like in other ceramics and understand the physical mechanisms behind the flash effect are analysed. The investigation allows to point out the importance of the fundamental processing variables like the applied pressure and voltage for obtain high density material. The key role of the starting particles' surface chemistry is identified to generate specific microstructures and determine peculiar physical and mechanical properties in the flash sintered ceramic.

### 1. Introduction

The first “official” paper [1] on flash sintering was published in 2010 by prof. Rishi Raj’s research group at the University of Colorado in Boulder (USA) and it describes that the application of a relatively high electrical field (60–120 V/cm) to a dog-bone-shaped sample of pressed zirconia (3YSZ) powder suspended in a furnace at temperature below 1100 °C is responsible for a very rapid densification occurring in less than 5 s. Since then, a real explosion of research activities has been recorded in several labs around the globe aiming at verifying the possibility to extend the observed phenomenon to other ceramics and understanding the physical and chemical mechanisms involved in the process for the development of a new low-energy-demanding production of ceramic materials [2–9].

It is now clear that flash sintering can be successfully applied to monolithic ceramics and composites characterized by a negative temperature coefficient (NTC) for electrical resistivity, i.e., to materials whose conductivity decreases with temperature [8,9]. Most of the research activities on flash sintering indicated that the fundamental mechanisms, which allow the extremely fast densification are associated to a thermal runaway phenomenon [9,10]; this occurs at a specific combination of temperature and applied electric field and is associated

with the sudden flow of electric current through the material, which induces its very rapid heating. Said phenomenon is possible because of the NTC nature of most ceramics, regardless of whether they are insulators, electronic conductors or semiconductors. Nevertheless, it is certainly attractive to extend flash sintering also to ceramics with metal-like electrical conductivity (therefore with positive temperature coefficient, PTC), these including materials with outstanding thermal, chemical and mechanical properties (for example, carbides and borides), which are notoriously difficult to be consolidated by conventional processes. Some isolated attempts carried out using spark plasma sintering apparatus on zirconium and titanium diboride [11,12] or more specific configurations for aluminium and tungsten are reported in the literature [13,14]. More recently, pressure-assisted flash sintering experiments using a moderate load (10–50 MPa) together with an electrical field were carried out successfully to densify highly conductive ceramics like hafnium-zirconium diborides [15] and various nitrides [16–19].

In the present overview, the results of a recent extensive investigation aiming at consolidating tungsten carbide and zirconium diboride by flash sintering are reported with the aim to identify the conditions for inducing a thermal runaway effect also in such metal-like ceramics, understand the physical mechanisms behind the flash phenomenon in

\* Corresponding author. Department of Industrial Engineering, University of Trento, via Sommarive 9, Trento, Italy.

E-mail address: [vincenzo.sglavo@unitn.it](mailto:vincenzo.sglavo@unitn.it) (V.M. Sglavo).

<sup>1</sup> Now at: Empa, Swiss Federal Laboratories for Materials Science and Technology, Überlandstrasse 129, CH-8600 Dübendorf, Zürich, Switzerland.

PTC materials, describe the fundamental structural and mechanical properties of the produced ceramics and point out possible limitations and future advancements. In order to introduce the matter, a short summary on flash sintering is anticipated here to make the differences between NTC and PTC materials clearer.

## 2. Flash sintering

Regardless the specific configuration used for the experiment (like the original one proposed by Cologna et al. [1] with a dog-bone-shaped specimen suspended in a tubular furnace by two metallic wires acting as electrodes or the simpler one where a pellet is placed within a modified dilatometer between two metallic disks connected to the power supply [9], very similar to the flash spark plasma sintering or microwave flash sintering – adapted equipment [5,20–23]) it is now clear that a specific combination of furnace temperature and applied field a certain current starts to flow along the material thus inducing very rapid heating of the pressed ceramic powder and consequent sintering [8,9,24].

The flash sintering phenomenon has been shown to occur using different modes (constant, monotonically or stepwise increasing) for changing the temperature or the electric field, in AC or DC. It typically consists of three fundamental stages: the first one where the ceramic sample behaves like an insulator and a limited (but not zero) current flows; the second one (specifically, the flash event) where, for a particular combination of furnace temperature and applied electrical field, the current density increases abruptly thus raising very quickly the sample temperature and leading to its very rapid densification; the third and last one, where, in order to prevent further increase of temperature and excessive current flow across the equipment, a maximum current density is set and the phenomenon can proceed in stationary conditions [9,24]. It is interesting to observe that the transition between the first and the second stage always occurs when the dissipated power is in the range 5–50 mW/mm<sup>3</sup>, irrespective of the composition and structure of the considered ceramic material.

Flash sintering occurrence can be recognized by some specific fingerprints. First of all, sintering appears simultaneously with a sudden drop in the specimen resistivity, the powder sample being subjected to very rapid heating (in the order of  $\approx 10^3$ – $10^4$  K/min); an evident bright light emission (like a “flash”) also accompanies the almost immediate shrinkage. Secondly, a minimum electrical conductivity is needed to produce the “flash”; in other words, flash sintering is not activated in perfectly electrically insulating materials. Finally, the onset temperature, alias the furnace temperature at which the phenomenon occurs, decreases with the applied electrical field. Here, an additional “universal” feature seems possible to be pointed out since some works have identified the Debye temperature as the minimum possible temperature for inducing the flash in any ceramic material, no matter how intense the applied electrical field is [25,26].

A certain number of mechanisms have been advanced to explain how flash sintering occurs. Starting from that less recognized, in some works the phenomenon was accounted for by a preferential Joule heating at the grain boundary due to the higher electrical resistance of this latter associated with more difficult diffusion processes and space charge formation [27–30]. This could lead to huge temperature gradients, overheating and, locally, grain boundary melting which can induce intense mass flux towards the neck among the particles and promote densification.

Some researchers also identified the formation of electrochemically partially reduced structures in oxides as a trigger for the activation of the flash event; in this way the material becomes partially electrically conductive and can also change its diffusion kinetics [31–35].

Another mechanism advanced to explain the flash phenomenon, sometimes referred as athermal effect [36], is the field-induced formation of Frenkel disorder in the material [37–41]; vacancies and interstitials are therefore generated, and these can then be ionized to produce free electrons and holes, which contribute to the electrical

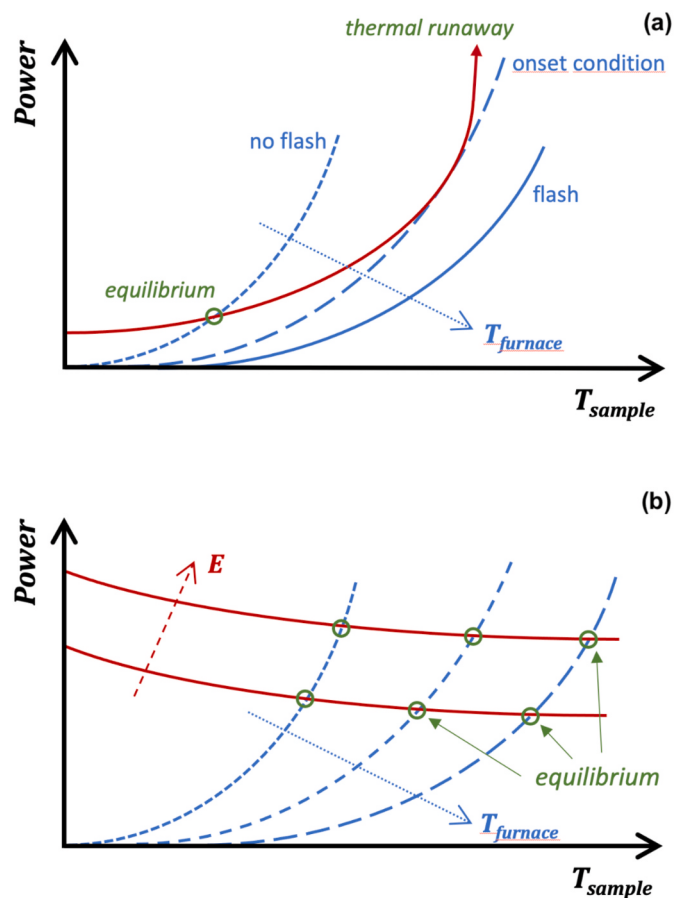


**Fig. 1.** Evolution of the electrical power generated by the current flux across the resistive ceramic (blue curves) and the power dissipated as heat from the surface of the specimen (red curves) as a function of the specimen temperature as the furnace temperature is increased: (a) for native NTC material under constant electric field; (b) for PTC material at variable electrical field. (For interpretation of the references to colour in this figure legend, the reader is referred to the Web version of this article.)

conductivity, vacancies and interstitials, which can have a role in improving the mass transport and, therefore, densification.

An additional athermal effect, where the electric field or current induce the acceleration of grain boundary diffusion with a reduced activation energy for plastic deformation, was also identified during high temperature flexural tests carried out on dense zirconia samples [36,42].

In any case, it is quite universally accepted that the fundamental mechanism behind flash sintering is the thermal runaway generated by Joule heating [8–10]; when the compacted powder sample is crossed by an electrical current its temperature increases and both electrical conduction and diffusion upsurge. A relatively simple model can be considered to describe the thermal runaway phenomenon; it is based on the balance between the electrical power generated by the current flux across the resistive ceramic ( $W_{in}$ ) and the power dissipated as heat from the surface of the specimen ( $W_{out}$ ). These two quantities can be expressed as [10]:

$$W_{in} = Vol \frac{E^2}{\rho} \quad (1)$$

$$W_{out} = Surf \epsilon \sigma_{SB} (T_s^4 - T_f^4) \quad (2)$$

where Vol and Surf are the volume and the external surface of the specimen, E the electric field,  $\rho$  the electrical resistivity,  $\epsilon$  the emissivity,

$\sigma_{SB}$  the Stefan & Boltzmann constant,  $T_s$  and  $T_f$  the temperature of the specimen and of the sample. It is therefore assumed that the heat is dissipated by radiation, only, as it is reasonable at relatively high temperature. At this point it is important to know how the resistivity of the material ( $\rho$ ) changes with temperature. Typically, ceramics show an Arrhenius-like electrical conduction [43]; in other words, the material is characterized by a negative temperature coefficient (NTC) for the electrical resistivity, which means that the resistivity decreases with the temperature. In such case, Eq. (1) becomes:

$$W_{in} = Vol \frac{E^2}{\rho_0} e^{-Q/RT_s} \quad (3)$$

$\rho_0$  being the pre-exponential factor for the resistivity,  $Q$  the activation energy for conduction and  $R$  the perfect gas constant.

The comparison of  $W_{in}$  and  $W_{out}$  and especially the generation of the flash event can be easily understood by using a graphical representation as in Fig. 1(a). The red curve represents the power generated by the current flux across the ceramic while the blue ones correspond to the power dissipated by radiation, these moving to the right as the furnace temperature increases. If  $T_f$  is relatively low (first blue curve on the left), an equilibrium condition is reached and the system/specimen is absolutely stable in terms of temperature. Nevertheless, by increasing the furnace temperature (middle blue curve), an onset condition is reached where the heat generated by the Joule effect can not be totally dissipated by radiation and the sample experiences a sudden heating, which induces the flash phenomenon. The onset condition can be easily determined in terms of critical electric field ( $E_c$ ) on the basis of Eqs (2) and (3) is one assumes also the tangency condition between  $W_{in}$  and  $W_{out}$  in Fig. 1:

$$E_c = \left[ \frac{4 p \epsilon \sigma_{SB} \rho_0 R}{S Q} T_c^5 e^{Q/RT_c} \right]^{0.5} \quad (4)$$

where  $p$  and  $S$  are the perimeter and the area of the cross section of the specimen and the temperature of this latter at the onset is

$$T_c = T_f + \Delta T_c \quad (5)$$

the excess temperature with respect to the furnace one being

$$\Delta T_c \approx \frac{R T_f^2}{Q - 5 R T_f} \quad (6)$$

A certain number of ceramics are characterized by an electrical resistivity which increases with temperature (the so-called PTC ceramics, with positive temperature coefficient for resistivity) as it occurs in metals [43]. Among them one can include several carbides or borides which are known for some outstanding properties like very high melting point, exceptional chemical resistance, hardness and elastic modulus, being therefore very important in some strategic applications. If one assumes a metal-like resistivity [43,44], Eq. (1) becomes:

$$W_{in} = Vol \frac{E^2}{\rho_i + \alpha T_s^m} \quad (7)$$

where  $m$  is a small positive number (equal to 1 above the Debye temperature),  $\rho_i$  and  $\alpha$  being two constants depending on the material. In this case, as shown in Fig. 1(b), there is always an equilibrium between  $W_{in}$  and  $W_{out}$  and, therefore, it is theoretically impossible to activate a thermal runaway phenomenon, i.e., to generate an intense energy useful for inducing a sufficient heating of the material for the activation of sintering processes. Therefore, for PTC ceramics, if the voltage is for example kept constant, very intense current and long times are necessary to promote the powders' consolidation.

In the past, similar conditions were used in electric current assisted sintering (ECAS) technologies (also called field-assisted sintering techniques, FAST) sporadically proposed for the densification of metals or cemented carbides; here a mechanical pressure was combined with an

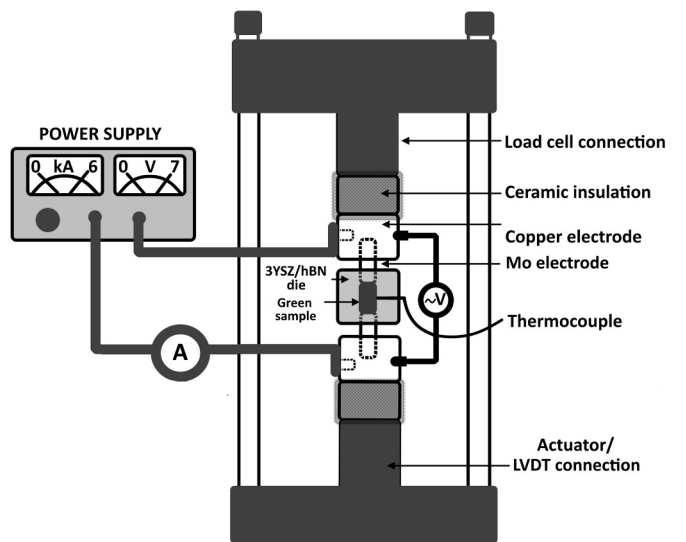


Fig. 2. Schematic of the apparatus used for the flash sintering experiments.

electrical current, which provided the required amount of resistive heat to promote particles bonding and densification. For example, in SPS (Spark Plasma Sintering), widely used to produce a variety of materials, ceramics and metals, relatively low current densities and voltages are applied (typically less than 10 V and around 1 kA/cm<sup>2</sup>) and the consolidation can occur in some minutes, thus requiring, in the case of metals or hard metals, the use of controlled atmosphere [45]. Conversely, in EDS (Electro Discharge Sintering) [46] and ERS (Electric Resistance Sintering) [47–49] higher current (>5 kA/cm<sup>2</sup>) which were limitedly applied for the consolidation of highly conductive metals or WC-Co cemented carbides and the process duration is of the order of a few seconds, thus allowing to operate in air. In both cases sintering must also be necessarily aided by the application of pressure, typically in the order of some hundreds of megapascal.

Previous copious experience on flash sintering of ceramics [7] and the cited germinal works on field-assisted sintering of metals and cemented carbides motivated the present authors to start a research work aiming at understanding whether similar techniques could be used to sinter metal-like ceramics in air atmosphere and in very limited time. The experimental procedures developed during the investigation to promote a flash sintering process on two very important metal-like ceramics like tungsten carbide and zirconium diboride are described in the following section. Then, the results in terms of material structure and mechanical properties are presented.

### 3. Experimental procedure

For the present work, commercially available powders were used: nanocrystalline tungsten carbide from Inframaterial Advanced Materials ( $D_{50} = 150$ –240 nm) and Grade B zirconium diboride from Höganäs ( $D_{50} = 1.5$ –3 µm). Two batches of WC nano-powder containing different oxide species content, ~1.2 wt% for the so called oxidized one and 0.3 wt% for the purest one as reported in previous works [50,51], were used. After unsuccessful preliminary tests, ZrB<sub>2</sub> powder was treated under Ar-5% H<sub>2</sub> at 800 °C for 2 h to reduce the content of surface oxidized species.

The powders were initially uniaxially pressed into cylindrical samples (diameter = 6 mm, height = 7 mm) under 350 MPa maximum pressure.

Flash sintering experiments were carried out using a custom-made apparatus shown in Fig. 2 where two copper/molybdenum electrodes were fastened to the load cell and the actuator piston connected to the displacement transducer (LVDT) of a universal mechanical testing

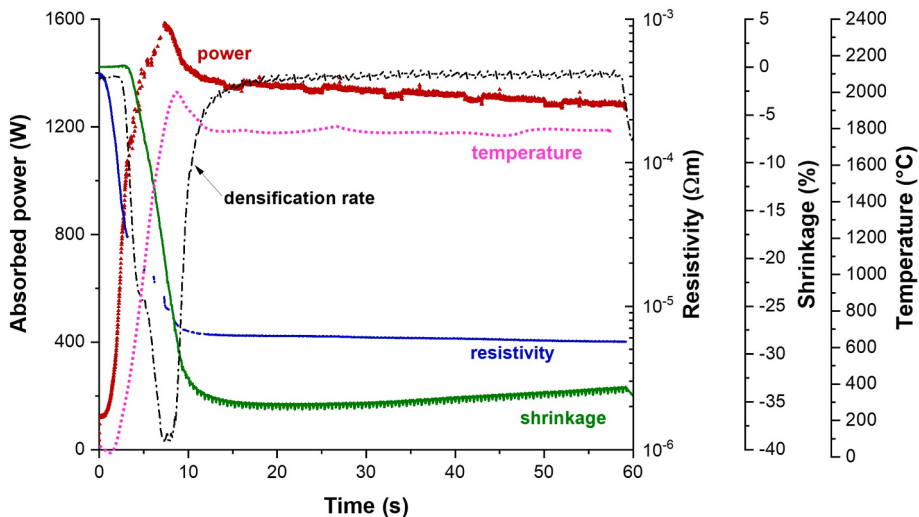


**Fig. 3.** Exemplary diagram of the sintering process phenomenology for a tungsten carbide sample initially subjected to 3.7 V under 4 MPa for a duration of 60 s. The densification rate is plotted using arbitrary units.

machine (MTS System, Mod. 810).

The green sample was compressed between the molybdenum electrodes while inserted into an electrically insulating die (made of 3YSZ or hBN). In this way the pressure applied to the specimen and its shrinkage during the process could be determined from the applied force and the displacement measured by the system controlling the machine. The electric power was provided using an AC 50 Hz power supply (TECNA item 3870) connected to the metallic electrodes [50].

Sintering treatments of 10 s–60 s were performed by applying pressures ranging from 4 MPa to 100 MPa and voltages from 3 V to 5 V. In the case of purest WC powders most of the investigations were carried out using 3.7 V and 4 MPa pressure, these conditions corresponding to the optimized ones after the extensive work performed using the other powder. Voltage and current across the samples were simultaneously measured upon sintering using a multichannel data acquisition system (DAQ NI USB 6211). The voltage measurement was performed between the Cu electrodes while the current was recorded by means of a calibrated shunt resistance (2500 A, 60 mV) placed in series with the system. Electrical data (voltage and current) were acquired and processed by a proprietary LabView software, which sampled the two current and voltage signals at 100 ksample/s, thus reconstructing the two 50 Hz sinusoidal signals without aliasing errors. The average electrical power dissipated within the ceramic sample, at a certain time step, was then evaluated under the assumption that the impedance of the green body was entirely resistive (zero phase shift). The resistivity evolution during the sintering tests could be therefore accurately assessed, considering

the initial thickness of the green pellet and its shrinkage.

The density of the sintered specimens was determined using the Archimedes' method following the ASTM C830 norm.

The WC sintered samples were then sectioned along the direction of the applied electric current and pressure and polished using diamond abrasive pastes to achieve a mirror-like surface. This allowed successive observation using a FE-SEM microscope (ThermoFisher® Apreo 2S LoVac). Micropillars (diameter = 3 μm, height = 6 μm) were produced on these polished surfaces using a FIB-SEM dual-column microscope (Helios NanoLab 600i) operating at 30 kV for micro-mechanical compression tests. The fabrication of the pillars involved a two-step process utilizing a concentric ring milling pattern: initially, a circular trench with the pillar at the centre was created using high FIB current (9.3 nA), followed by a reduction of the pillar's tapering angle to less than 3.5° under lower current (0.23 nA) [52]. Micro-compression tests under displacement control (6 nm/s) were carried out at room temperature using Hysitron triboindenter TI950 equipped with a 15 μm diameter flat punch diamond indenter [52].

Vickers indentations were produced on the surface of polished WC specimens to measure hardness and fracture toughness. This latter was calculated from the measurement of the radial cracks' length using a digital optical microscope (Olympus DSX1000) using the well-known Anstis et al. formula [53].

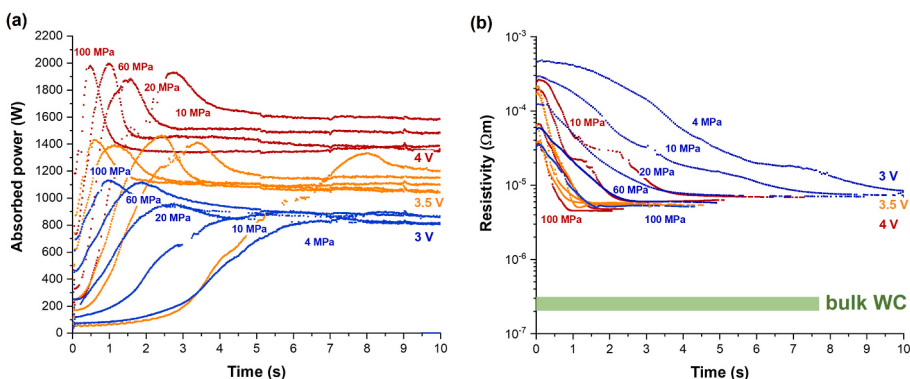


**Fig. 4.** Evolution of the (a) absorbed power and (b) resistivity for 10 s long flash sintering experiments on WC samples subjected to different pressure and initial voltage. The resistivity range for bulk WC is shown for comparison.

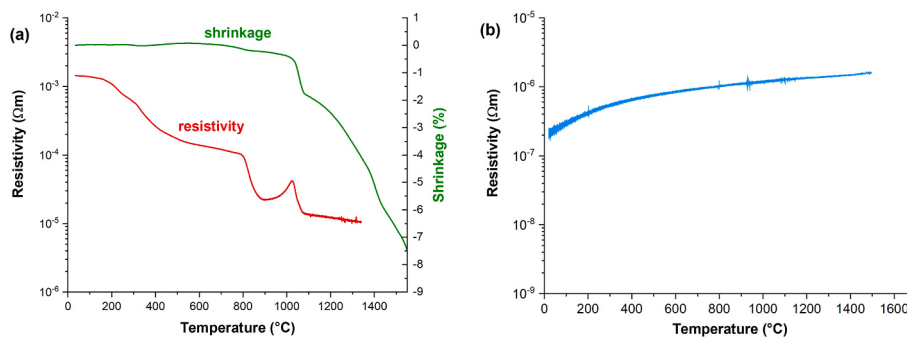


**Fig. 5.** Resistivity as a function of temperature for (a) green WC pellet and (b) fully dense material. The shrinkage of the sample upon heating is also shown in (a). (For interpretation of the references to colour in this figure legend, the reader is referred to the Web version of this article.)

#### 4. Results and discussion

Fig. 3 shows an exemplary diagram which summarizes the phenomenology of the sintering process of a sample initially subjected to 3.7 V electrical potential and 4 MPa pressure for a duration of 60 s [50]. One can at first observe that in slightly more than 10 s the sample shrinks of about 35 %, thus pointing out an evident and very rapid densification; as a matter of fact, the obtained specimen was characterized by a relative density in excess of 95 %. Within the same time interval, the absorbed power and temperature quickly increase and then remain substantially constant while the resistivity of the pellet decreases by about two orders of magnitude. Interestingly, the densification rate shows a maximum in correspondence of the highest power absorption value.

All these observations allow to state that the recorded phenomenon can be compared in all aspects to a flash sintering process: the electrical resistivity decreases quite rapidly while density increases, an evident peak in the absorbed power and temperature is recorded and the densification rate is maximum at the power peak; in addition, the densification occurs under the effect of very high heating rate which can be estimated in about 10.000–20.000 °C/min. This is exactly what one can observe during the flash sintering of any other NTC ceramic material.

One feature which deserves to be analysed in certain detail is the influence of the applied pressure, this representing a potential additional densification promoter with respect to typical flash sintering experiments [54]. Fig. 4 shows how the absorbed power and the resistivity evolve during the first 10 s of the process. From a qualitative point of view, the absorbed power initially increases with a rate which scales with the applied load, the maximum being reached in very short time (<2 s) at the highest pressures. Correspondingly, the resistivity decreases more rapidly when the pressure is high. It is useful to point out here that the final plateau reached by the measured resistivity at about 5·10<sup>-6</sup> Ω m is associated with the minimum sensitivity of the measuring system and not with the real material behaviour. Probably one of the fundamental data in Fig. 4 is that, at very low pressure, the initial resistivity of the green sample is about three orders of magnitude larger than that measured on bulk tungsten carbide, which is around 10<sup>-6</sup>–10<sup>-7</sup> Ω m as it will be also discussed below [50]. Also the effect of the applied voltage is very clear in Fig. 4, determining an increase of the absorbed power and reducing the time necessary for the resistivity to reach the minimum value. In addition, if one combines the temperature evolution from Fig. 2 with the resistivity one in Fig. 4(b), it is straightforward that the green compact is characterized by a NTC behaviour at the beginning of the process. As a matter of fact, Fig. 5 shows the evolution of resistivity measured on fully dense tungsten carbide and on a green WC sample. In this case, the conductivity was measured in a four-point configuration using a digital multimeter (Keithley DMM 6500) on a sample placed within the dilatometer (Linseis, L75 PT). The bulk sample was produced starting from the oxidized powder by SPS

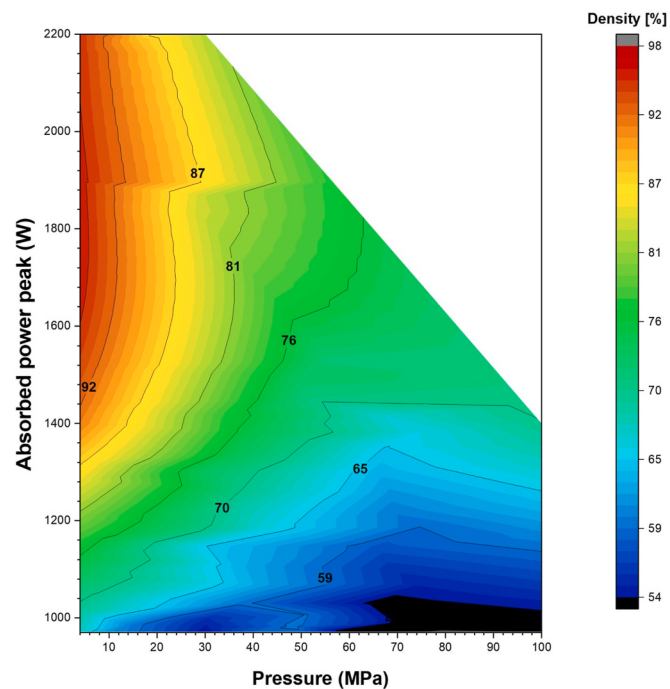


**Fig. 6.** Process map of the density achieved for variable absorbed power and applied pressure values in 10 s long flash sintering experiments carried out using the oxidized WC powder.

(Dr. Sinter 1050) at 2100 °C [50]; the green specimen was instead identical to those used for the flash sintering experiments. As expected, bulk material shows an increasing resistivity with temperature (PTC behaviour) while in the green compact the resistivity clearly decreases. Also, the absolute values are substantially different, the resistivity of fully dense WC being one-to-three orders of magnitude smaller with respect to the green compact. It is also interesting to observe that, this latter case, the evolution is not monotonic especially at about 800 °C and 1000 °C. The correlation of the resistivity evolution with the recorded shrinkage can help in identifying the involved phenomena. Initially, the particles constituting the green specimen form a very loose network, where the limited contact points account for the very high resistivity [55]. As the temperature increases, two phenomena can occur: first, the, although limited, surface diffusion processes can determine an expansion of the extension of said contact points; second, at high temperature an evolution of the particles' surface chemistry can occur, for example with the decomposition of oxides or hydroxides which act as resistive layers. Both phenomena are anyway responsible for a reduction of the green compact resistivity. Similar effects were identified also by Eskandariyun et al. [19] and especially by Gibson et al. [56] who

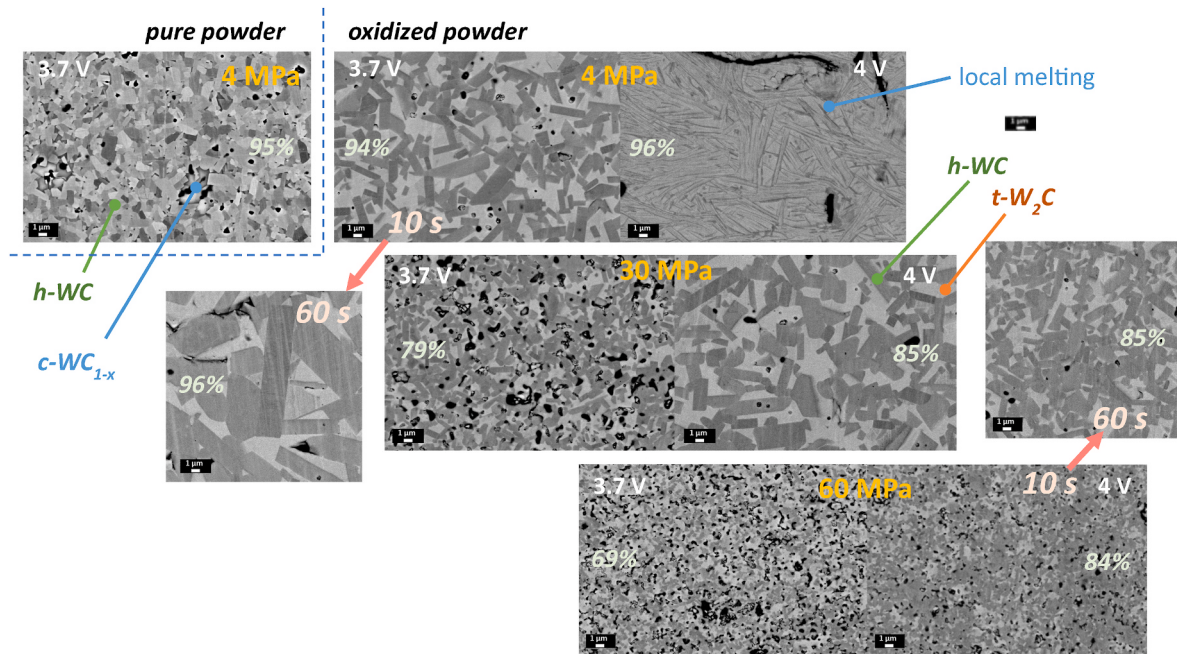


**Fig. 7.** Microstructure of the WC materials produced by flash sintering from pure (top left, only) and oxidized powder under different applied pressure (4, 30 and 60 MPa) and initial applied voltage (3.7 and 4 V); the evolution of the structure when the process lasts for 60 s instead of 10 s is also shown. For all the specimens the relative density is indicated. The different mineralogical phases generated in the materials obtained starting from pure and oxidized powder are specified.

identified similar undulation in the resistivity vs. temperature plot and attributed them to the removal of surface resistive layers.

Based on the arguments discussed above, the importance of the applied pressure appears clear; it has a fundamental role in the determination of the initial resistivity since it determines the extension of the contact area among the particles. Therefore, for a given material, the overall evolution of the sintering process depends substantially on the initial applied load and voltage, which, in turn, determine the evolution of the electrical power/energy available for the densification of the green compact. The results of several investigations carried out using the oxidized WC powder [50,54] are shown in Fig. 6 in terms of final density as function of the applied pressure and absorbed power peak. One can easily observe, quite surprisingly, that only for limited pressure and higher electrical potential, relative density larger than 90 % can be achieved in 10 s.

The observations performed so far lead to two fundamental comments. The first regards the resistivity evolution. As said, the green sample shows a decreasing resistivity like in a NTC ceramic and this behaviour can be accounted for by an extrinsic effect in native PTC material correlated with the granular structure of the specimen where the contact points among the particles are initially limited and grow as densification proceeds. Very similar arguments were also proposed by Gibson et al. for the flash sintering of SiC [56]. They pointed out that the NTC of silicon carbide was too weak to explain the observed thermal runaway-driven flash event, which was instead originated in the early stages of sintering when improved connectivity among the particles led to a resistivity reduction. Therefore, one can assume that the extrinsic NTC behaviour observed here is the cause of a thermal runaway phenomenon, whose intensity and duration depend on the applied pressure (fundamental for determining the contact points extension) and the voltage (this determining the power which is absorbed by the sample and used for the densification). Consequently, as anticipated before, a fundamental and unusual compromise is realized between the applied pressure and the sintering behaviour during the flash sintering of an electronic conductor ceramic like tungsten carbide. If the green pellet is subjected to relatively high load, the contact among the particles is initially wider and this makes the resistivity initially lower; the thermal

runaway can be promoted but its duration is short, and the available energy (product of the power and time) is not enough to guarantee complete densification. Conversely, when the applied pressure is limited, a larger amount of energy is made available for completing the sintering process. When the voltage/pressure combination becomes critical, the temperature can be as high as the melting point of the material as shown in Fig. 7 [54]. The surface and, especially, the surface chemistry of WC particles play an important role in the flash sintering process fundamentally because they determines the electrical properties (above all, resistivity) at the contact points among the powders. Therefore, it is not surprising that different microstructures are obtained by using powders whose surface is chemically dissimilar as will be specified below [51].

Another aspect is related to the very high heating rate, which is developed by the thermal runaway activated because of the extrinsic NTC behaviour of the powder compact. In agreement with previous results reported in the literature [57], there is no doubt that the very efficient densification observed here must be correlated with the huge temperature gradient generated in the specimen until its resistivity remains relatively high. Regardless of the applied pressure and voltage used in the present experiments, the heating rate is always in the order of  $10^4$  °C/min or more [50] and this is anyway more than enough for determining very efficient densification [57].

Not only the density but also the microstructure of the material depends on the processing conditions (voltage and applied pressure) [50, 51,54]. As shown in Fig. 7 a biphasic structure was always produced by using the oxidized powder, consisting of hexagonal WC phase (darker) and trigonal W<sub>2</sub>C one, the extension of each microconstituent increasing with the energy (and temperature) involved upon flash sintering as pointed out before. In addition, when the holding time is increased, a coarsening of the grains is promoted with a certain evolution also of the density. The situation changes dramatically when non-oxidized WC powder is used [58]. In this case, the material is almost completely consisting of hexagonal WC phase with limited amount of sub-stoichiometric metastable cubic WC<sub>1-x</sub> phase, the presence of this latter being correlated with the ultrafast sintering process carried out using a powder with specific surface chemistry [58]. This confirms the

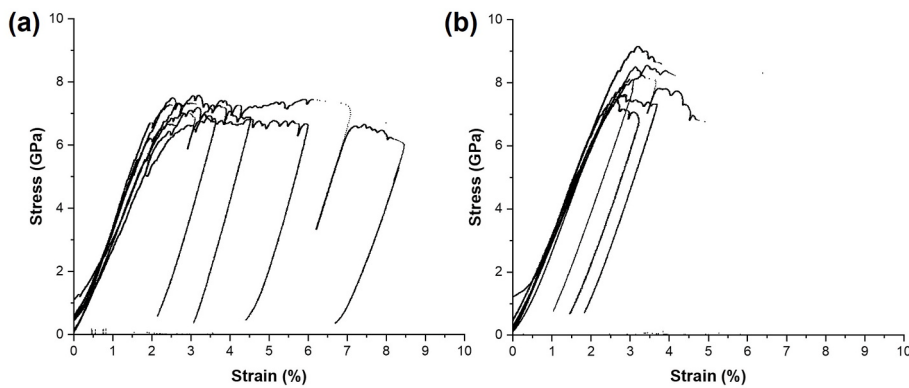


**Fig. 8.** Stress-strain curves recorded during micro-compression tests carried out at room temperature on flash sintered WC produced by using (a) oxidized and (b) pure powder.

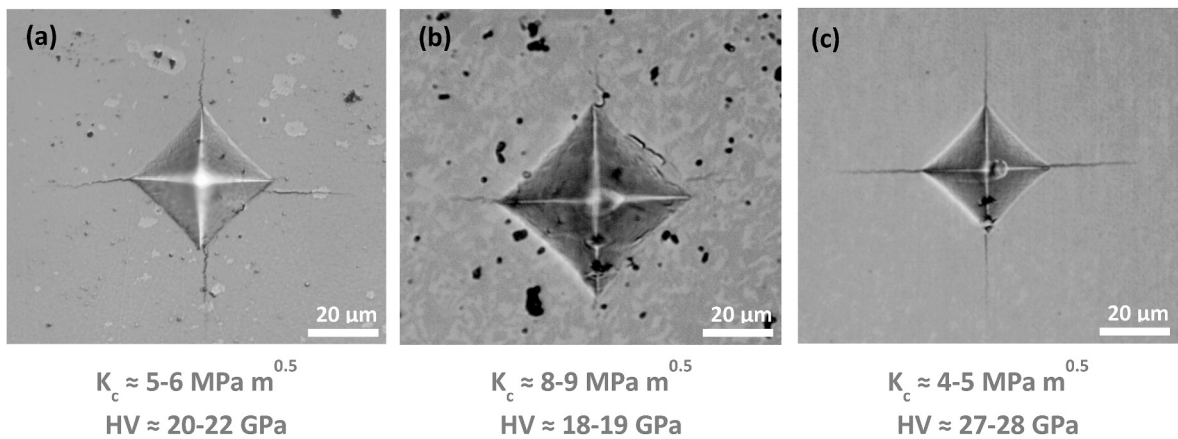


**Fig. 9.** Vickers indentation imprint at 19.8 N maximum load, hardness and fracture toughness of WC specimens produced by using (a) pure and (b) oxidized powder. A micrograph and corresponding data for a WC specimen produced with oxidized powder by SPS is also shown (c).

importance of the powders' surface chemistry in the sintering behaviour of ceramics [59]. A detailed analysis of the XRD line broadening performed on the spectra collected on the different WC materials allowed the quantification of the lattice defects, which turned out to be extremely abundant especially in the W<sub>2</sub>C phase, which was identified in samples produced both by oxidized and non-oxidized powder [52,58], and largely more present than in analogous materials produced for example by SPS or conventional sintering. Although the nature of the defects (vacancies or dislocations) can not be distinguished by the used methodology, for sure they have a key role in the grain growth kinetics of the flash sintered tungsten carbide [52,58]. Overall, one can state that these results point out the possibility to produce different microstructures in flash sintered tungsten carbide starting from powders with dissimilar surface chemistry and using variable processing conditions.

The specific biphasic structure generated in the flash sintered WC materials has some important effects on their mechanical behaviour. Fig. 8 shows the stress-strain curves recorded during micro-compression tests carried out at room temperature on pillars produced within a FIB-SEM microscope. One can observe the different microplasticity of the two materials, that produced by the pure powder appearing definitely more brittle but stiffer and stronger; micro-pillars produced instead starting from oxidized powder can reach very high strains (5–9 %) without failure with an evident plastic deformation [52].

The described micro-mechanical behaviour also has some fundamental consequences on the macro-mechanical performances as shown in Fig. 9; tungsten carbide produced by flash sintering starting from oxidized powder is characterized by a slightly lower hardness but much higher fracture toughness, the obtained values appearing very

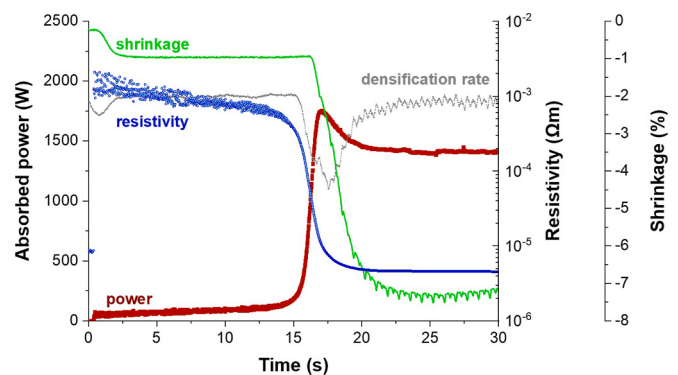


**Fig. 10.** Exemplary diagram of the sintering process phenomenology for a zirconium diboride sample initially subjected to 3.7 V under 5 MPa. The densification rate is plotted using arbitrary units.

interesting especially if compared to tungsten carbide produced by SPS [60]. The peculiar behaviour of flash sintered WC, and especially that produced starting from oxidized powder, can be accounted for by the peculiar microstructure which can allow the activation of toughening mechanisms like grain bridging and crack deflection [60]. These results appear particularly important since they demonstrate the possibility of tailoring the mechanical properties of pure tungsten carbide produced by flash sintering starting from specific powders and using well identified processing conditions.

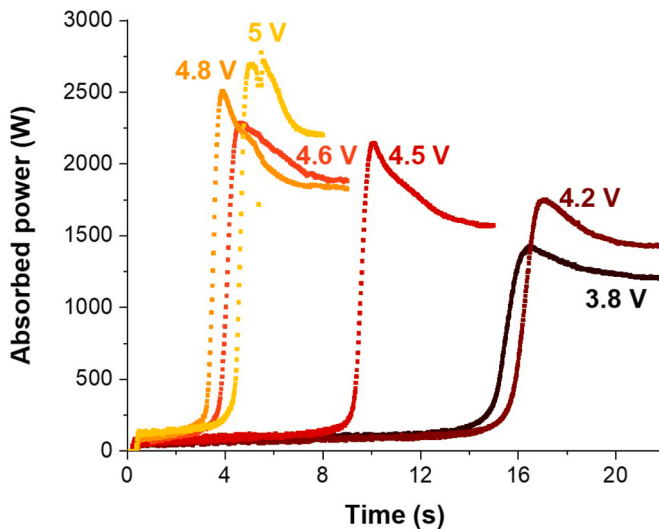


**Fig. 11.** Absorbed power as a function of the initial voltage for the flash sintering of  $\text{ZrB}_2$ .

As well as in tungsten carbide, the surface chemistry was revealed to be fundamental also in the flash sintering of another native PTC ceramic like zirconium diboride. When the as-purchased powder was used, the sintering processes were hardly reproducible and large variation in density and microstructure was recorded. Conversely, when the powder was preliminarily treated in  $\text{Ar}/\text{H}_2$ , thus removing most of the surface oxides, sintering could be controlled to a much higher extent and interesting results were obtained. This confirms some previous findings regarding the powders' surface chemistry importance in the consolidation by hot pressing or SPS of  $\text{ZrB}_2$  ceramics [61,62]. An exemplary diagram reporting the fundamental parameters of the flash sintering of  $\text{ZrB}_2$  is shown in Fig. 10. Differently from tungsten carbide, an incubation time is always recorded although, once activated, the flash phenomenon occurs in the same way with an abrupt increase of the absorbed power in correspondence of the resistivity drop thus determining the shrinkage to occur in less than 10 s. The origin of the incubation stage has not been clarified yet, but it could be correlated with the evolution of the surface layers' chemistry to reach the favourable condition for proper electrical conduction. Also in the present case, the applied voltage represents a fundamental processing variable, determining the intensity of the absorbed power peak and the delay of the appearance of this latter as shown in Fig. 11: as the voltage is increased, the flash phenomenon is anticipated and the power peak increases.

Correspondingly, the densification of the material changes as summarized in Fig. 12. The density of the produced materials is not outstanding reaching in the best cases about 77 %. Here the applied pressure seems to play a slightly different role with respect to what reported before for tungsten carbide; one can in fact observe that the application of a limited pressure (10–20 MPa) has a positive effect on the final density.

In any case the reported result must be discussed based on two fundamental aspects: first of all, the starting powder is definitely coarse with grains as big as  $5 \mu\text{m}$ , clearly not optimal for sintering processes; secondly, the overall duration of the process is always very short. Some preliminary results have already indicated that the use of specific sintering additives (like, for example the same tungsten carbide) or a slightly longer process (up to 1 min) can determine much higher density values, up to 90 %.

One final comment can be made regarding the power associated with the activation of the thermal runaway phenomenon. As said before, in NTC ceramics the transition between stage I (incubation) and stage II (thermal runaway) of flash sintering always occurs when the dissipated power is in the range 5–50 mW/mm<sup>3</sup>, regardless the composition and structure of the considered material. In case of native PTC ceramics like tungsten carbide and zirconium diboride, one can calculate the specific absorbed power necessary to activate the thermal runaway from the temperature and power data like in Fig. 3 and for all the experiments carried out so far it is in the order of 10–20 W/mm<sup>3</sup>, about three orders larger than in NTC ceramics. This probably represents an additional fingerprint of the flash sintering of PTC compounds, which can also be correlated with the fact that in such materials, stage II is also limited by the “extrinsic NTC → PTC” transition. The physical explanation of the very different power associated to the thermal runaway is not straightforward. One aspect which could be considered is that in NTC materials the charge carriers are atoms which are also the species participating to diffusion and sintering. Conversely, in PTC ceramics, the charge carriers are electrons which, instead, do not contribute to mass transport and, therefore, an extra energy is needed for moving the atoms. Additional investigations are clearly needed to address such additional aspects.

## 5. Conclusions

Both tungsten carbide and zirconium diboride can be successfully produced by flash sintering by using optimized processing conditions in very short time (less than a minute). Final microstructure, density and mechanical properties (like hardness and fracture toughness) depend on three fundamental processing parameters like surface chemistry of the starting powder, applied pressure and voltage.

Sintering behaviour is correlated with a thermal runaway phenomenon generated by the extrinsic NTC behaviour of the powder compact

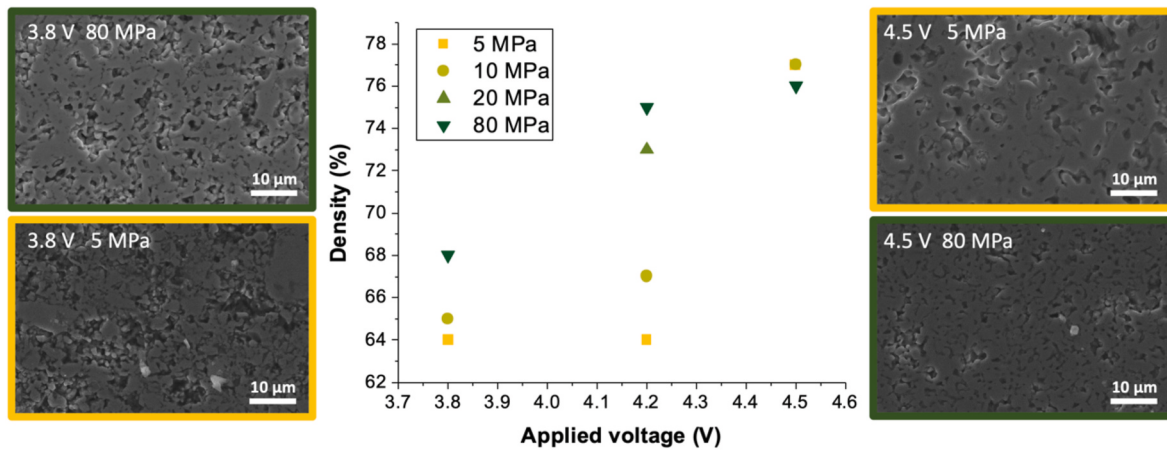


**Fig. 12.** Relative density of the flash sintered  $\text{ZrB}_2$  specimens as a function of the applied voltage and pressure. The microstructure of the material is also shown by the micrographs.

at the beginning of the process although the considered materials are intrinsically PTC (positive temperature coefficient for resistivity) like metals. Surface chemistry of the starting powder and pressure play a fundamental role in the densification behaviour since they determine the initial electrical resistance of the powder compact and, therefore, influence the power which is initially dissipated in the material to activate the diffusional phenomena necessary for sintering. The very efficient densification must be also associated to the enormous temperature gradient generated in the powder compact until its resistivity remains relatively high.

The results presented in the present work greatly expand the potentiality of flash sintering as an efficient, low-energy intensity process for metals and, especially, hard ceramics.

### CRediT authorship contribution statement

**Vincenzo M. Sglavo:** Conceptualization, Formal analysis, Funding acquisition, Project administration, Resources, Supervision, Writing – original draft, Writing – review & editing. **Emanuele De Bona:** Data curation, Investigation, Writing – original draft. **Isacco Mazo:** Data curation, Formal analysis, Investigation, Methodology, Writing – original draft.

### Declaration of competing interest

The authors declare that they have no known competing financial interests or personal relationships that could have appeared to influence the work reported in this paper.

### Acknowledgements

The University of Trento is acknowledged for the financial support.

### References

- [1] M. Cologna, B. Rashkova, R. Raj, Flash sintering of nanograin zirconia in <5 s at 850°C, *J. Am. Ceram. Soc.* 93 (2010) 3556–3559, <https://doi.org/10.1111/j.1551-2916.2010.04089.x>.
- [2] M. Biesuz, V.M. Sglavo, Beyond flash sintering: how the flash event could change ceramics and glass processing, *Scripta Mater.* 187 (2020) 49–56, <https://doi.org/10.1016/j.scriptamat.2020.05.065>.
- [3] M. Biesuz, V.M. Sglavo, Flash sintering of ceramics, *J. Eur. Ceram. Soc.* 39 (2019) 115–143, <https://doi.org/10.1016/j.jeurceramsoc.2018.08.048>.
- [4] M. Biesuz, S. Grasso, V.M. Sglavo, What's new in ceramics sintering? A short report on the latest trends and future prospects, *Curr. Opin. Solid State Mater. Sci.* 24 (2020) 100868, <https://doi.org/10.1016/j.cossms.2020.100868>.
- [5] C.E.J. Dancer, Flash sintering of ceramic materials, *Mater. Res. Express* 3 (2016) 102001, <https://doi.org/10.1088/2053-1591/3/10/102001>.
- [6] H. Zhou, X. Li, Y. Zhu, J. Liu, A. Wu, G. Ma, X. Wang, Z. Jia, L. Wang, Review of flash sintering with strong electric field, *High Volt.* 7 (2022) 1–11, <https://doi.org/10.1049/hve2.12080>.
- [7] E. Gil-González, L.A. Pérez-Maqueda, P.E. Sánchez-Jiménez, A. Perejón, Flash sintering research perspective: a bibliometric analysis, *Materials* 15 (2022) 416, <https://doi.org/10.3390/ma15020416>.
- [8] R.I. Todd, Flash sintering of ceramics: a short review, in: Proceedings of the IV Advanced Ceramics and Applications Conference, Atlantis Press, Paris, 2017, pp. 1–12, [https://doi.org/10.2991/978-94-6239-213-7\\_1](https://doi.org/10.2991/978-94-6239-213-7_1).
- [9] M. Biesuz, V.M. Sglavo, Flash sintering of ceramics, *J. Eur. Ceram. Soc.* 39 (2019), <https://doi.org/10.1016/j.jeurceramsoc.2018.08.048>.
- [10] R.I. Todd, E. Zapata-Solvas, R.S. Bonilla, T. Sneddon, P.R. Wilshaw, Electrical characteristics of flash sintering: thermal runaway of Joule heating, *J. Eur. Ceram. Soc.* 35 (2015) 1865–1877, <https://doi.org/10.1016/j.jeurceramsoc.2014.12.022>.
- [11] R. McKinnon, S. Grasso, A. Tudball, M.J. Reece, Flash spark plasma sintering of cold-Pressed TiB<sub>2</sub> · h BN, *J. Eur. Ceram. Soc.* 37 (2017) 2787–2794, <https://doi.org/10.1016/j.jeurceramsoc.2017.01.029>.
- [12] S. Grasso, T. Saunders, H. Porwal, O. Cedillos-Barraza, D.D. Jayaseelan, W.E. Lee, M.J. Reece, Flash Spark Plasma Sintering (<sc>FSPS</sc>) of Pure <sc>ZrB</sc> <sc>ZrB</sc><sub>2</sub>, *J. Am. Ceram. Soc.* 97 (2014) 2405–2408, <https://doi.org/10.1111/jace.13109>.
- [13] B. McWilliams, J. Yu, F. Kellogg, Sintering aluminum alloy powder using direct current electric fields at room temperature in seconds, *J. Mater. Sci.* 53 (2018) 9297–9304, <https://doi.org/10.1007/s10853-018-2207-6>.
- [14] E. Bamidele, S.I.A. Jalali, A.W. Weimer, R. Raj, Flash sintering of tungsten at room temperature (without a furnace) in <1 min by injection of electrical currents at different rates, *J. Am. Ceram. Soc.* 107 (2024) 817–829, <https://doi.org/10.1111/jace.19532>.
- [15] J. Belisario, S. Mondal, I. Khakpour, A. Franco Hernandez, A. Durygin, Z. Cheng, Synthesis and flash sintering of (Hf<sub>1-x</sub>Zr<sub>x</sub>)B<sub>2</sub> solid solution powders, *J. Eur. Ceram. Soc.* 41 (2021) 2215–2225, <https://doi.org/10.1016/j.jeurceramsoc.2020.12.015>.
- [16] S. Das, D. Dubois, M.S.I. Sozal, Y. Emirov, B. Jafarizadeh, C. Wang, V. Drozd, A. Durygin, Z. Cheng, Synthesis and flash sintering of zirconium nitride powder, *J. Am. Ceram. Soc.* 105 (2022) 3925–3936, <https://doi.org/10.1111/jace.18421>.
- [17] S. Das, A. Durygin, V. Drozd, M.S.I. Sozal, Z. Cheng, Reactive flash sintering of TiZrN and TiAlN ternary metal nitrides, *J. Eur. Ceram. Soc.* 44 (2024) 2037–2051, <https://doi.org/10.1016/j.jeurceramsoc.2023.11.079>.
- [18] S. Mondal, A. Durygin, V. Drozd, J. Belisario, Z. Cheng, Multicomponent bulk metal nitride (Nb<sub>1/3</sub>Ta<sub>1/3</sub>Ti<sub>1/3</sub>)N<sub>1-δ</sub> synthesis via reaction flash sintering and characterizations, *J. Am. Ceram. Soc.* 103 (2020) 4876–4893, <https://doi.org/10.1111/jace.17226>.
- [19] A. Eskandariyoun, S. Das, D. Dubois, K. Saeedian, A. Durygin, V. Drozd, Z. Cheng, Effects of processing conditions on flash sintering of commercial ZrN, *J. Am. Ceram. Soc.* (2024), <https://doi.org/10.1111/jace.19719>.
- [20] S. Grasso, T. Saunders, H. Porwal, B. Milsom, A. Tudball, M. Reece, Flash spark plasma sintering (<sc>FSPS</sc>) of α and β SiC, *J. Am. Ceram. Soc.* 99 (2016) 1534–1543, <https://doi.org/10.1111/jace.14158>.
- [21] C. Manière, G. Lee, E.A. Olevsky, All-materials-inclusive flash spark plasma sintering, *Sci. Rep.* 7 (2017) 15071, <https://doi.org/10.1038/s41598-017-15365-x>.
- [22] C. Manière, G. Lee, T. Zahrah, E.A. Olevsky, Microwave flash sintering of metal powders: from experimental evidence to multiphysics simulation, *Acta Mater.* 147 (2018) 24–34, <https://doi.org/10.1016/j.actamat.2018.01.017>.
- [23] E.A. Olevsky, S.M. Rolfig, A.L. Maximenko, Flash (Ultra-Rapid) spark-plasma sintering of silicon carbide, *Sci. Rep.* 6 (2016) 33408, <https://doi.org/10.1038/srep33408>.
- [24] M. Yu, S. Grasso, R. McKinnon, T. Saunders, M.J. Reece, Review of flash sintering: materials, mechanisms and modelling, *Adv. Appl. Ceram.* 116 (2017) 24–60, <https://doi.org/10.1080/17436753.2016.1251051>.
- [25] T.P. Mishra, V. Avila, R.R.I. Neto, M. Bram, O. Guillou, R. Raj, On the role of Debye temperature in the onset of flash in three oxides, *Scripta Mater.* 170 (2019) 81–84, <https://doi.org/10.1016/j.scriptamat.2019.05.030>.
- [26] D. Yadav, R. Raj, Two unique measurements related to flash experiments with yttria-stabilized zirconia, *J. Am. Ceram. Soc.* 100 (2017) 5374–5378, <https://doi.org/10.1111/jace.15114>.
- [27] R. Chaim, C. Estournès, On thermal runaway and local endothermic/exothermic reactions during flash sintering of ceramic nanoparticles, *J. Mater. Sci.* 53 (2018) 6378–6389, <https://doi.org/10.1007/s10853-018-2040-y>.
- [28] R. Chaim, G. Chevallier, A. Weibel, C. Estournès, Flash sintering of dielectric nanoparticles as a percolation phenomenon through a softened film, *J. Appl. Phys.* 121 (2017), <https://doi.org/10.1063/1.4980853>.
- [29] J. Narayan, A new mechanism for field-assisted processing and flash sintering of materials, *Scripta Mater.* 69 (2013) 107–111, <https://doi.org/10.1016/j.scriptamat.2013.02.020>.
- [30] G. Corapcioglu, M.A. Gulgun, K. Kisslinger, S. Sturm, ShikharK. Jha, R. Raj, Microstructure and microchemistry of flash sintered K<sub>0.5</sub>Na<sub>0.5</sub>NbO<sub>3</sub><sub>3</sub><sub>3</sub>, *J. Ceram. Soc. Jpn.* 124 (2016) 321–328, <https://doi.org/10.2109/jcersj2.15290>.
- [31] M. Biesuz, L. Pinter, T. Saunders, M. Reece, J. Binner, V. Sglavo, S. Grasso, Investigation of electrochemical, optical and thermal effects during flash sintering of 8YSZ, *Materials* 11 (2018) 1214, <https://doi.org/10.3390/ma11071214>.
- [32] H. Yoshida, P. Biswas, R. Johnson, M.K. Mohan, Flash-sintering of magnesium aluminate spinel (MgAl<sub>2</sub>O<sub>4</sub>) ceramics, *J. Am. Ceram. Soc.* 100 (2017) 554–562, <https://doi.org/10.1011/jace.14616>.
- [33] H. Yoshida, K. Morita, B.-N. Kim, Y. Sakka, T. Yamamoto, Reduction in sintering temperature for flash-sintering of yttria by nickel cation-doping, *Acta Mater.* 106 (2016) 344–352, <https://doi.org/10.1016/j.actamat.2016.01.037>.
- [34] H. Charalambous, S.K. Jha, X.L. Phuah, H. Wang, H. Wang, J.S. Okasinski, T. Tsakalakos, In situ measurement of temperature and reduction of rutile titania using energy dispersive x-ray diffraction, *J. Eur. Ceram. Soc.* 38 (2018) 5503–5511, <https://doi.org/10.1016/j.jeurceramsoc.2018.08.032>.
- [35] H. Charalambous, S.K. Jha, H. Wang, X.L. Phuah, H. Wang, T. Tsakalakos, Inhomogeneous reduction and its relation to grain growth of titania during flash sintering, *Scripta Mater.* 155 (2018) 37–40, <https://doi.org/10.1016/j.scriptamat.2018.06.017>.
- [36] H. Yoshida, Control of high temperature mass transport phenomena through grain boundaries in oxide ceramics based on grain boundary chemical composition and external electric field, *J. Ceram. Soc. Jpn.* 130 (2022) 22070, <https://doi.org/10.2109/jcersj2.22070>.
- [37] J.S.C. Francis, R. Raj, Flash-sinterforging of nanograin zirconia: field assisted sintering and superplasticity, *J. Am. Ceram. Soc.* 95 (2012) 138–146, <https://doi.org/10.1111/j.1551-2916.2011.04855.x>.
- [38] R. Raj, M. Cologna, J.S.C. Francis, Influence of externally imposed and internally generated electrical fields on grain growth, diffusional creep, sintering and related phenomena in ceramics, *J. Am. Ceram. Soc.* 94 (2011) 1941–1965, <https://doi.org/10.1111/j.1551-2916.2011.04652.x>.
- [39] J.G. Pereira da Silva, J. Lebrun, H.A. Al-Qureshi, R. Janssen, R. Raj, Temperature distributions during flash sintering of 8% yttria-stabilized zirconia, *J. Am. Ceram. Soc.* 98 (2015) 3525–3528, <https://doi.org/10.1111/jace.13786>.
- [40] M. Jongmanns, R. Raj, D.E. Wolf, Generation of Frenkel defects above the Debye temperature by proliferation of phonons near the Brillouin zone edge, *New J. Phys.* 20 (2018) 093013, <https://doi.org/10.1088/1367-2630/aadd5a>.

- [41] J.-M. Lebrun, C.S. Hellberg, S.K. Jha, W.M. Kriven, A. Steveson, K.C. Seymour, N. Bernstein, S.C. Erwin, R. Raj, In-situ measurements of lattice expansion related to defect generation during flash sintering, *J. Am. Ceram. Soc.* 100 (2017) 4965–4970, <https://doi.org/10.1111/jace.15071>.
- [42] H. Motomura, D. Tamao, K. Nambu, H. Masuda, H. Yoshida, Athermal effect of flash event on high-temperature plastic deformation in Y2O3-stabilized tetragonal ZrO<sub>2</sub> polycrystal, *J. Eur. Ceram. Soc.* 42 (2022) 5045–5052, <https://doi.org/10.1016/j.jeurceramsoc.2022.04.055>.
- [43] C.B. Carter, M.G. Norton, Ceramic materials: Science and engineering. <https://doi.org/10.1007/978-1-4614-3523-5>, 2013.
- [44] Charles Kittel, *Introduzione Alla Fisica Dello Stato Solido*, third ed., 1986 (in Italian), Boringhieri, Torino.
- [45] U. Anselmi-Tamburini, J.E. Garay, Z.A. Munir, Fundamental investigations on the spark plasma sintering/synthesis process, *Mater. Sci. Eng., A* 407 (2005) 24–30, <https://doi.org/10.1016/j.msea.2005.06.066>.
- [46] A. Fais, Processing characteristics and parameters in capacitor discharge sintering, *J. Mater. Process. Technol.* 210 (2010) 2223–2230, <https://doi.org/10.1016/j.jmatprotec.2010.08.009>.
- [47] J.M. Montes, J.A. Rodríguez, F.G. Cuevas, J. Cintas, Consolidation by electrical resistance sintering of Ti powder, *J. Mater. Sci.* 46 (2011) 5197–5207, <https://doi.org/10.1007/s10853-011-5456-1>.
- [48] M.A. Lagos, I. Agote, T. Schubert, T. Weissgaerber, J.M. Gallardo, J.M. Montes, L. Prakash, C. Andreouli, V. Oikonomou, D. Lopez, J.A. Calero, Development of electric resistance sintering process for the fabrication of hard metals: processing, microstructure and mechanical properties, *Int. J. Refract. Metals Hard Mater.* 66 (2017) 88–94, <https://doi.org/10.1016/j.ijrmhm.2017.03.005>.
- [49] J. Shon, J. Park, K. Cho, J. Hong, N. Park, M. Oh, Effects of various sintering methods on microstructure and mechanical properties of CP-Ti powder consolidations, *Trans. Nonferrous Metals Soc. China* 24 (2014) s59–s67, [https://doi.org/10.1016/S1003-6326\(14\)63289-1](https://doi.org/10.1016/S1003-6326(14)63289-1).
- [50] I. Mazo, A. Molinari, V.M. Sglavo, Electrical resistance flash sintering of tungsten carbide, *Mater. Des.* 213 (2022) 110330, <https://doi.org/10.1016/j.matdes.2021.110330>.
- [51] I. Mazo, L.E. Vanzetti, J.M. Molina-Aldareguia, A. Molinari, V.M. Sglavo, Role of surface carbon nanolayer on the activation of flash sintering in tungsten carbide, *Int. J. Refract. Metals Hard Mater.* 111 (2023) 106090, <https://doi.org/10.1016/j.ijrmhm.2022.106090>.
- [52] I. Mazo, M.A. Monclus, J.M. Molina-Aldareguia, V.M. Sglavo, Does flash sintering alter the deformation mechanisms of tungsten carbide? *Acta Mater.* 258 (2023) 119227 <https://doi.org/10.1016/j.actamat.2023.119227>.
- [53] G.R. Anstis, P. Chantikul, B.R. Lawn, D.B. Marshall, A critical evaluation of indentation techniques for measuring fracture toughness: I, direct crack measurements, *J. Am. Ceram. Soc.* 64 (1981) 533–538, <https://doi.org/10.1111/j.1151-2916.1981.tb10320.x>.
- [54] I. Mazo, A. Molinari, V.M. Sglavo, Effect of pressure on the electrical resistance flash sintering of tungsten carbide, *J. Eur. Ceram. Soc.* 42 (2022) 2028–2038, <https://doi.org/10.1016/j.jeurceramsoc.2022.01.017>.
- [55] A. Mikrajuddin, F.G. Shi, H.K. Kim, K. Okuyama, Size-dependent electrical constriction resistance for contacts of arbitrary size: from Sharvin to Holm limits, *Mater. Sci. Semicond. Process.* 2 (1999) 321–327, [https://doi.org/10.1016/S1369-8001\(99\)00036-0](https://doi.org/10.1016/S1369-8001(99)00036-0).
- [56] A. Gibson, Y. Li, R.S. Bonilla, R.I. Todd, Pressureless flash sintering of  $\alpha$ -SiC: electrical characteristics and densification, *Acta Mater.* 241 (2022) 118362, <https://doi.org/10.1016/j.actamat.2022.118362>.
- [57] W. Ji, B. Parker, S. Falco, J.Y. Zhang, Z.Y. Fu, R.I. Todd, Ultra-fast firing: effect of heating rate on sintering of 3YSZ, with and without an electric field, *J. Eur. Ceram. Soc.* 37 (2017) 2547–2551, <https://doi.org/10.1016/j.jeurceramsoc.2017.01.033>.
- [58] I. Mazo, J.M. Molina-Aldareguia, A. Molinari, V.M. Sglavo, Room temperature stability, structure and mechanical properties of cubic tungsten carbide in flash sintered products, *J. Mater. Sci.* 58 (2023) 1829–1848, <https://doi.org/10.1007/s10853-022-08109-4>.
- [59] P. Badica, S. Grasso, H. Borodianska, S.S. Xie, P. Li, P. Tatarko, M.J. Reece, Y. Sakka, O. Vasylkiv, Tough and dense boron carbide obtained by high-pressure (300 MPa) and low-temperature (1600°C) spark plasma sintering, *J. Ceram. Soc. Jpn.* 122 (2014) 271–275, <https://doi.org/10.2109/jcersj2.122.271>.
- [60] I. Mazo, M.A. Monclus, J.M. Molina-Aldareguia, V.M. Sglavo, Fracture resistance of binderless tungsten carbide consolidated by spark plasma sintering and flash sintering, *Open Ceramics* 17 (2024) 100533, <https://doi.org/10.1016/j.oceram.2023.100533>.
- [61] W.-W. Wu, G.-J. Zhang, Y.-M. Kan, Y. Sakka, Synthesis, microstructure and mechanical properties of reactively sintered ZrB<sub>2</sub>–SiC–ZrN composites, *Ceram. Int.* 39 (2013) 7273–7277, <https://doi.org/10.1016/j.ceramint.2013.02.028>.
- [62] T. Mizuguchi, S. Guo, Y. Kagawa, Transmission electron microscopy characterization of spark plasma sintered ZrB<sub>2</sub> ceramic, *Ceram. Int.* 36 (2010) 943–946, <https://doi.org/10.1016/j.ceramint.2009.10.025>.